LAWRENCE
LIVERMORE
NATIONAL
LABORATORY

LLNL-JRNL-451192

Novel Three-Dimensional Networks of SnO2 Nanoslabs: Synthesis and Their Sensing Response to NO2

S. Mueng, S. -W. Kim, D. -H. Lee, S. -E. Moon, S. -H. Kim, D. H. Yoon, A. Maiti, J. W. Gardner, F. Udrea, W. I. Milne

August 26, 2010

ACS Applied Materials and Interfaces

Disclaimer

This document was prepared as an account of work sponsored by an agency of the United States government. Neither the United States government nor Lawrence Livermore National Security, LLC, nor any of their employees makes any warranty, expressed or implied, or assumes any legal liability or responsibility for the accuracy, completeness, or usefulness of any information, apparatus, product, or process disclosed, or represents that its use would not infringe privately owned rights. Reference herein to any specific commercial product, process, or service by trade name, trademark, manufacturer, or otherwise does not necessarily constitute or imply its endorsement, recommendation, or favoring by the United States government or Lawrence Livermore National Security, LLC. The views and opinions of authors expressed herein do not necessarily state or reflect those of the United States government or Lawrence Livermore National Security, LLC, and shall not be used for advertising or product endorsement purposes.

Novel Three-Dimensional Networks of SnO_2 Nanoslabs: Synthesis and their Sensing Response to NO_2

Sunglyul Maeng,[*,†] Sang-Woo Kim,[**,‡] Deuk-Hee Lee,[‡] Seung-Eon Moon,[§] Sang-Hyeob Kim,[§] Dae Ho Yoon,[‖] Amitesh Maiti, [***,⊥] Julian W. Gardner,[#] Florin Udrea,[▼] and William I. Milne[▼]

IT Convergence Research Laboratory, Woosuk University, Samrye-Eup, Wanju-Gun, Jeonbuk, 565-701, Korea, School of Advanced Materials and System Engineering, Kumoh National Institute of Technology, 1 Yangho-dong, Gumi, Gyeongbuk, 730-701, Korea, IT Convergence Technology Research Division, Electronics and Telecommunications Research Institute, 161 Gajeong-dong, Yuseong, Daejeon, 305-700, Korea, Department of Advanced Materials Engineering and SAINT, Sungkyunkwan University, Suwon, Gyeonggi, 440-746, Korea, Lawrence Livermore National Laboratory, Livermore, CA 94551,USA, School of Engineering, University of Warwick, Coventry, CV4 7AL, UK, and Department of Engineering, University of Cambridge, 9 JJ Thomson Ave, Cambridge, CB30FA, UK

† IT Convergence Research Laboratory, Woosuk University.

‡ School of Advanced Materials and System Engineering, Kumoh National Institute of Technology.

§ IT Convergence Technology Research Division, Electronics and Telecommunications Research Institute.

‖ Department of Advanced Materials Engineering and SAINT, Sungkyunkwan University.

⊥ Lawrence Livermore National Laboratory.

School of Engineering, University of Warwick.

▼Department of Engineering, University of Cambridge.

[*,**] The authors contributed equally to this work.

[*,**,***] Corresponding authors.

E-mail: sunglyulm@gmail.com (S. Maeng); kimsw@kumoh.ac.kr (S.-W. Kim); amaiti@llnl.gov(A. Maiti).

Graphic for the Table of Contents

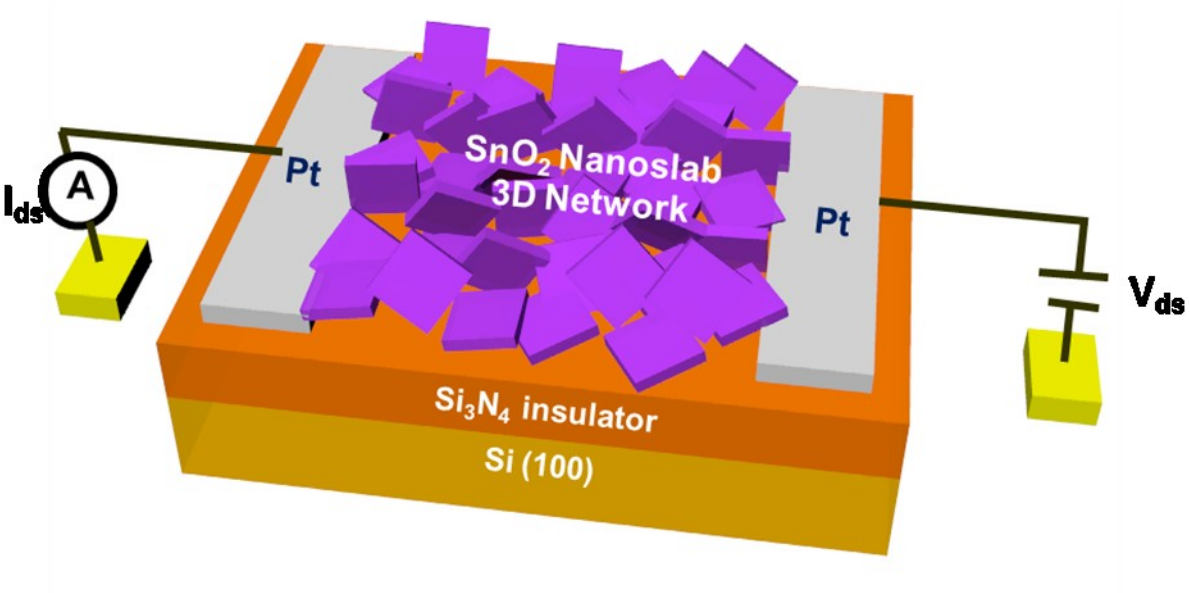

ABSTRACT

We report the formation of a self-assembled three-dimensional network of tetragonal SnO nanoslabs by simple thermal evaporation at 500˚C directly onto Pt interdigited electrode-patterned Si_3N_4/Si substrates, followed by the complete transformation into a stable rutile SnO_2 network through thermal annealing at 700 ˚C for 2.5 hours. No catalyst or vacuum environment was required in such synthesis. The chemical gating effects of such network device were tested with various concentrations of NO_2 gas. At operating temperatures of 300 ˚C orders of magnitude change in nanoslab conductance was observed even for sub-ppm concentrations of NO_2. By studying the dependence of sensor response on NO_2 concentration we deduce that at these operating temperatures the key kinetic mechanism involves the binding of NO_2 molecules to surface O-vacancies of the SnO_2 slabs. We develop analytical equations relating sensor response to partial charge transfer between the analyte and exposed SnO_2 surfaces and show that our experimental observations are in quantitative consistency with charge-transfer values obtained from first-principles computation.

KEYWORDS: SnO_2 nanoslab; three-dimensional network; thermal evaporation; chemical gating; NO_2 gas sensing; flat band condition

Solid state *n*-type semiconductors, metal oxides in general, and tin dioxide (SnO_2) in particular, have been widely exploited as gas sensors. The sensing mechanism relies on interactions between adsorbed gas molecule (adsorbate) and the semiconductor surface. The adsorbate acts as extrinsic surface states and the electron exchange between the surface states and the bulk takes place within a surface layer with thickness of the order of the Debye length λ_D. If the adsorbate has oxidizing (reducing) character it tends to capture (release) electrons. If the size (thickness) of the semiconductor is comparable to $\sim \lambda_D$, most of the conduction electrons can be possibly captured from (released to) the surface by the extrinsic surface states, which can lead to the orders of magnitude conductance change.[1-6] This reaction, termed as *chemical gating*, can be compared to the electrostatic gating in field effect transistor (FET), which exhibits orders of magnitude of conductance change under electrostatic gate voltage modulation. Conventional gas sensors have the capability of detecting parts per million (ppm) concentrations of gaseous species. However, chemical gating effects enable us to detect down to parts per billion (ppb) concentrations of analytes, a typical requirement for the next generation sensors.

For sensors based on quasi zero-dimensional (0D) ultrafine SnO_2 nanocrystals, dramatic change in electrical conductance has been reported when the size of a nanoparticle less than 10 nm.[3,7-11] However, sensors with ultrafine grain size are known to exhibit poor long-term stability. Grain coalescence inevitably occurs during the high temperature cycles of calcination or sensor operation.[8,12] Such structural instability has impeded the widespread application of sensors based on quasi-0D nanocrystalline materials.

Various authors have reported that nanostructures with higher dimensions are much more stable under high temperature conditions. Fabrications of monolayer quasi-one dimensional (1D)

nanostructured semiconductor sensors have been extensively investigated in various ways such as nano-patterning of thin layer,[13] direct lateral growth using pre-patterned catalyst,[14-16] surface-programmed monolayer assembly,[17] and dielectro-phoresis.[18,19] Most of the above-mentioned techniques, however, involve many detailed, expensive steps such as nanolithography, pre-deposition and patterning of the catalyst, introduction of a self-assembled monolayer, or utilization of microchannels. For commercial feasibility of gas sensing applications, it is very important to develop processes involving simple, easy and minimal fabrication steps.

Recently, Quasi-1D,[20-23] 2D,[24,25] and three-dimensional (3D)[5] semiconductor nanosenors fabricated by the drop coating technique have been reported. In such a method, the nanostructured sensing material is first dispersed in liquid to form a suspension. Then, the suspension is drop-coated onto the interdigitated area of the electrodes. Even though the technique is simple and cost-effective, uniform dispersion is difficult due to strong van der Waals forces. Thus, agglomeration of nanostructures is inevitable,[24] which leads to low sensitivity, slow response, and more importantly poor reproducibility.

In this letter, we report for the first time the *in situ* fabrication of a standing 3D network of SnO_2 nanoslabs by a very simple and cost-effective thermal evaporation technique. We also establish the theoretical models necessary for the analysis of the sensing response to NO_2 gas. This enabled us to deduce the key chemical gating mechanism, and helped achieve quantitative consistency between the observed sensing behavior and the partial charge transfer previously computed by first-principles Density Functional Theory (DFT).

For the fabrication of the 3D network of sensors, we first formed 100 nm thick Pt interdigitated electrode (IDE) on Si_3N_4/Si (001) substrate by e-beam evaporation. *In situ* growth of tin sub-oxide (SnO) nanoslabs was then carried out by thermal evaporation directly onto the substrate maintained at 500 °C in air. After the synthesis, post-thermal annealing was performed at 700 ^{o}C for 2.5 hour in an Ar environment. Figure 1a shows a schematic diagram of the sensor device. The plan-view field-emission scanning electron microscopy (FE-SEM) images of SnO nanoslab networks on the Pt IDE-patterned substrate are shown in Figures 1b,c. These two images illustrate that the interconnected standing SnO nanoslabs are packed only in the region between the Pt electrodes. From the images, the lateral, the vertical, and the thickness dimensions of a nanoslab can be estimated to be ~1 μm, ~1 μm, and ~100 nm, respectively.

The X-ray diffraction (XRD, RIGAKU D/MAX-2500) data were analyzed using a standard diffractometer with Cu Kα radiation in the θ-2θ configuration. The structural characterization of tin oxide was also carried out by transmission electron microscopy (TEM, FE-TEM FEI TM G2 F30) equipment. The as-synthesized tin oxide sample was identified as tetragonal SnO structure with a lattice constant of $a = b = 3.796$ Å and $c = 4.816$ Å as determined by XRD and TEM. However, upon annealing at 700 ^{o}C the XRD pattern changed. The new pattern, as shown in Figure 2a was in clear correspondence with a rutile SnO_2 structure with space group $P4_2/mnm$, and lattice parameters $a = b = 4.738$ Å and $c = 3.188$ Å.[26] The high-resolution TEM (HR-TEM) image of Fig. 2b also reveals a single crystalline phase with a rutile structure having no planar dislocations. The corresponding fast Fourier transformation (FFT) pattern (Figure 2b inset) further indicates that the SnO_2 nanoslab has the (101) face primarily exposed with preferred growth directions along [010] and $[10\bar{1}]$

respectively. The composition of the SnO_2 (101) surface can vary depending on the equilibrium conditions with the gas phase.[27]

In the following we investigate the sensing response of the (101) surface with a specific analyte, i.e., NO_2, one of the most frequently studied oxidizing gases. In the literature, NO_2 detection experiments by SnO_2 sensors have mostly been performed in air.[14, 16, 19, 28] In such case, the NO_2 is in competition with O_2 in adsorbing onto the surface of SnO_2, which complicates the analysis of the oxidation kinetics. To eliminate oxygen in our study, we mixed the test gas with N_2 to achieve the desired concentration and maintained the flow rate at 1000 standard cubic centimeter per minute (sccm) using a Bronkhorst High-Tech B.V. mass flow controllers (EL-FLOW series). The conductance of the device was measured by using an Agilent digital multimeter (model No.34411A) and a Keithley electrometer (model No. 6517A). The device shows non-linear current-voltage (I-V) characteristics at room temperature due to the back-to-back Schottky-like configuration. However, Ohmic behavior has been reported to become predominant over 200 ^{o}C.[29] In order to minimize influences from the Pt/SnO_2 contact we performed the NO_2 sensing experiments at 300 ^{o}C. Results of the conductance change of the nanoslab sensor upon cyclical exposure to NO_2 at different concentrations are shown in Figure 3. Noticeable drop in conductance is discernible even at NO_2 levels as low as 500 ppb, with significant drops at higher concentrations.

Figure 4 shows a low resolution cross-TEM image of a SnO_2 nanoslab network prepared by focused ion beam (FIB). As shown in this image, the SnO_2 nanoslabs synthesized in our experiments were mostly standing rather than lying. In an all-standing configuration, the NO_2 binding occurs on both sides of the slab. Thus, the gating characteristics should be comparable to a Fin- FET, where the channel potential is controlled more tightly than its planar counterpart.[30] Given that the length L and

width W of the nanoslabs (~1μm) are much larger than the depth D (~100 nm), each slab can be approximated as a 1D-layered (lamellar) structure. Solving the 1D Poisson equation with appropriate boundary conditions yields the relation $\Delta E/(k_B T) \sim [D/(\sqrt{8}\lambda_D)]^2$ (see Supporting Information) where ΔE is the potential energy difference between the center and surface of the nanoslab, and λ_D the Debye length. When ΔE is comparable with the thermal energy, it leads to a homogeneous electron concentration in the slab, which in turn results in the flat band case.[31] This happens for $\lambda_D \geq D/\sqrt{8}$ ~ 35 nm. Such Debye lengths are indeed attained at our experimental temperatures of T ~300 °C. In the inert gas (N_2) environment, the nanoslab behaves like a quasi-conductive element, while upon exposure to NO_2 almost all the electrons in the nanoslab are free to move to be captured by surface acceptors, leading to significant conductance drops. The schematic diagram explaining the operation of the SnO_2 nanoslab network NO_2 sensor is shown in the Figure 5.

For an n-type semiconductor gas sensor, the *response S* to an oxidizing gas is generally defined as $R/R_o - 1 = G_o/G - 1$, where R_o and G_o denote the initial resistance and conductance value respectively. For $G_o \gg G$, $S \approx G_o/G$. The sensor response as a function of NO_2 concentration is plotted in Figure 6. Under flat band condition, such response is known to assume a power law behavior.[2,32,33] Our data nicely fits the model $S = K_{NO_2} \cdot C_{NO_2}^{\alpha}$, where K_{NO_2} is a proportionality constant, C_{NO_2} is the NO_2 gas concentration, and the exponent $\alpha \approx 0.69$.

We now develop a theoretical model to relate exponent γ to electronic charge transfer from the SnO_2 surface to an adsorbed NO_2. Let us assume a NO_2 molecule adsorbed (physisorbed or chemisorbed) onto an available surface site S_{unocc} on the (101) surface with a net withdrawal of β electrons from the surface. Such process can be represented as:

$$NO_2^{gas} + \beta.e^- + S_{unocc} = NO_{2,S} \ , \quad (1)$$

where $NO_{2,S}$ represents a surface-adsorbed NO_2. By using the mass action law one obtains:

$$k_{ads} \cdot P_{NO_2} \cdot n_s^{\beta} \cdot [S_{unocc}] = k_{des} \cdot [NO_{2,S}] \ , \quad (2)$$

where n_s is the electron density at the surface (and is a function of the surface concentration of adsorbates) , P_{NO_2} is the gas pressure in the chamber, k_{ads} and k_{des} are reaction constants, and […] denotes surface density. Note that under the flat band condition, n_s is the homogeneous concentration of electrons throughout the whole SnO_2 nanoslab. The surface coverage of adsorbed NO_2 is defined as $\theta = [NO_{2,S}]/[S_{tot}]$, where $[S_{tot}] = [NO_{2,S}] + [S_{unocc}]$ is the total density of surface binding sites for NO_2. Thus, eq. (2) can be written as:

$$k_{ads} \cdot P_{NO_2} \cdot n_s^{\beta} \cdot (1-\theta) = k_{des} \cdot \theta \ , \quad (3)$$

If n_b is the electron density for the pristine material (i.e. $\theta = 0$), the condition of electrical neutrality yields the relation: $\beta \cdot \theta \cdot [S_{tot}].area + n_s \cdot volume = n_b \cdot volume$, where *area* and *volume* relate to total exposed (101) surface area and the total volume of the nanoslab respectively. In terms of surface adsorbate coverage (θ) the charge neutrality condition can be re-written as:

$$\theta = (n_b \cdot volume).(1 - n_s / n_b)/(\beta \cdot [S_{tot}].area) \ , \quad (4)$$

Since the SnO_2 slabs were not doped with impurities, the main source of the bulk conduction electrons are O-vacancies. As the bulk O-vacancies are shallow donors, essentially one electron is given up by each bulk O vacancy. Thus, we can assume that the bulk conduction electron density n_b is the same as the density of bulk O-vacancy [$V_{O,b}$]. Since all these electrons can be potentially taken up by surface adsorbate sites (see discussion on Debye length above), significant drops in

conductance can occur only when $\beta.[S_{tot}].area \approx (n_b.volume)$. Under these conditions, eq. (4) implies that:

$$\theta = 1 - n_s / n_b \tag{5}$$

Inserting eq. (5) into eq. (2) under conditions of large conductance drops, i.e., $n_b \gg n_s$ one obtains:

$$n_s \approx \{(k_{des} \cdot n_b) / k_{ads}\}^{\frac{1}{1+\beta}} \cdot P_{NO_2}^{-\frac{1}{1+\beta}} \tag{6}$$

Since $C_{NO_2} \propto P_{NO_2}$, it follows from eq. (6) that the sensor sensitivity $S \approx n_b / n_s \propto C_{NO_2}^{1/(1+\beta)}$, which implies that response exponent γ is related to the charge transfer β through the equation:

$$\alpha = \frac{1}{1+\beta} \tag{7}$$

Our experimental value of $\alpha = 0.69$ (see Fig. 6) corresponds to a charge transfer $\beta = 0.45$. Such a large charge transfer is usually indicative of a strong binding, e.g., as in chemisorption. Such strong binding is also consistent with the fact that after each desorption cycle the nanoslab conductance does not restore fully to its original pristine value before the introduction of any adsorbate (see Fig. 3).

In order to relate such binding to specific atomistic mechanisms, we refer to the existing literature. For instance, binding energies of NO_2 to the $(10\bar{1})$ surface of SnO_2 (which is chemically equivalent to the (101) surface for a rutile structure) and corresponding charge transfers for various configurations were computed by Maiti et al.[34] using DFT. Table 1 summarizes the computed binding energy and charge transfer for important adatom structures resulting from NO_2 to the $(10\bar{1})$ surface of SnO_2. The computed charge transfer of 0.51 el due to the binding of NO_2 to a surface O-vacancy corresponds well to 0.45 el charge transfer observed in our experiments. This would also be consistent with our high operation temperature of 300 ^{o}C at which a large concentration of surface O-

vacancies is likely[35-38] regardless of the method of synthesis. However, for direct comparisons of charge transfer between experiment and theory one needs to exert caution, given the dependence of computed charge transfer on the exchange-correlation functional and the partitioning schemes employed.[39] In addition, one needs to identify the amount of charge transfer due to the capture of conduction electrons as discussed here, versus that due to reorganization of valence electrons due to local chemical re-bonding, which mandates further analysis.

Finally, we also performed the above analysis on the mechanism in which NO_3 is formed by two NO_2 molecules through a disproportionation reaction on the (101) surface.[38] For this mechanism we obtain the relation $\alpha = 2/(1+\beta)$ (see Supporting Information). This cannot explain the observed value of α with any reasonable value of the charge transfer, and the vacancy mechanism appears more likely for the sensing response of our nanoslabs.

In summary, we have synthesized 3D networks of standing SnO_2 nanoslab gas sensors by employing a simple and cost-effective thermal deposition process for the first time. From observations of orders-of-magnitude conductance drops and theoretical calculations it was confirmed that the sensor acts as conductance switch in which a flat band condition is reached at 300 ˚C through double chemical gating by NO_2. The observed relationship between the sensor response and the NO_2 gas concentration was explained by assuming chemisorption of NO_2 molecules at a large number of O-vacancy sites on the predominantly exposed (101) surface of the SnO_2 nanoslabs.

ACKNOWLEDGMENT

This work has been partly supported by the RIC program of MKE in Woosuk University. This work also has been partly supported by the Korea Research Foundation Grant funded by the Korean

Government (MOEHRD, Basic Research Promotion Fund) (KRF-2008-331-D00294). The work by one of the authors (A. M.) was performed under the auspices of the U.S. Department of Energy by Lawrence Livermore National Laboratory under Contract DE-AC52-07NA27344.

REFERENCES

[1] Morrison, S.R., *The Chemical Physics of surfaces*; Plenium: New York, **1997**.

[2] Barsan, N.; Weimar, U., *J. Electroceram.* **2001**, *7*,143

[3] Epifani, M.; Diaz, R.; Arbiol, J.; Comini, E.; Sergent, N.; Pagnier, T.; Siciliano, P.; Faglia, G.; Morante, J.R., *Adv. Funct. Mater.* **2006**, *16*, 1488

[4] Kolmakov, A.; Zhang, Y.; Cheng, G.; Moskovits, M., *Adv.Mater.***2003**, *15*, 997

[5] Ponzoni, A.; Comini, E.; Sberveglieri, G.; Zhou, J.; Deng, S.Z.; Xu, N.S.; Ding, Y.; Wang, Z.L., *Appl. Phys. Lett*. **2006**, *88*, 203101.

[6] Wan, Q.; Li, Q.H.; Chen, Y.J.; Wang, T.H.; He, X.L.; Li, J.P.; Lin, C.L., *Appl. Phys. Lett*. **2004**, *84*, 3654

[7] Xu, C.; Tamaki, J.; Miura, N; Yamazoe, N., *Sens. Actuators B* **1991**, *3*, 147.

[8] Lu, F.; Liu, Y.; Dong, M.; Wang, X., *Sens. Actuators* B **2000**, *66*, 225.

[9] Demarane, V. ; Grisel, A., *Sens. Actuators B* **1993**, *15-16*, 63.

[10] Barsan N. ; Schweizer-Berberich, M. ; Gopel, W., *Fresenius J. Annal. Chem.* **1999**, *365,* 287.

[11] Chiu, H.-C.; Yeh, C.-S., *J.Phys.Chem.***2007**,*111*,7256

[12] Kholmanov, I.N. ; Barborini, E. ; Vinati, S. ; Piseri, P. ; Podesta, A. ; Ducati, C. ; Lenardi, C. ; Milani, P., *Nanotechnology* **2003**, *14*, 1168.

[13] Candeloro, P. ; Comini, E.; Baratto, C.; Faglia, G.; Sberveglieri, G., *J.Vac. Sci. Techol. B* **2005**, *23*, 2784

[14] Fruhberger, B.; Stirling, N.; Grillo, F.G.; Ma, S.; Ruthven, D.; Lad, R.J.; Frederick, B.G., *Sens. Actuators B* **2001**, *76*, 226.

[15] Law, M. ; Kind, H. ; Messer, B. ; Kim, F. ; Yang, P., *Angrew. Chem. Int. Ed*., **2002**, *41*, 2405.

[16] Huang, L. ; Wind, S.J. ; O'Brien, S.P. ; *Nano Lett*. **2003**, *3*, 299.

[17] Maeng, S.; Moon,S.; Kim, S.-H. ; Lee, H.-Y.; Park, S.-J.; Kwak, J.-H.; Park, K.-H.; Park, J.;Choi, Y.;Udrea, F.; Milne, W.I.;Lee, B.Y.; Lee, M.;Hong, S., *Appl. Phys. Lett*. **2008**, *93*, 113111.

[18] Kumar, S. ; Rajaraman, S. ; Gerhardt, R.A. ; Wang, J.L. ; Hesketh, P.J., *Electrochem. Acta,* **2005**, *51*, 943.

[19] Suehiro, J.; Imakire, H.; Hidaka, S.-I.; Weidong, D.; Guangbin, Z.; Imasaka, K.; Hara, M., *Sens. Actuators B,* **2006**, *114*, 943.

[20] Qi, P. ; Vermesh, O. ; Grecu, M. ; Javey, A. ; Wang, Q. ; Dai, H., *Nano Lett***. 2003**, *3*, 347.

[21] Maeng, S.; Moon,S.; Kim, S.-H. ; Lee, H.-Y.; Park, S.-J.; Kwak, J.-H.; Park, K.-H.; Park, J.;Choi, Y.;Udrea, F.; Milne, W.I.;Lee, B.Y.; Lee, M.;Hong, S., *Appl. Phys. Lett*. **2008**, *93*, 113111.

[22] Zhang, D. ; Liu, Z. ; Li, C. ; Tang, T. ; Liu, X. ; Han, S. ; Lei, B. ; Zhou, C., *Nano Lett*. **2004**, *4*, 1919.

[23] Comini, E. ; Faglia, G. ; Sberveglieri, G. ; Pan, Z. ; Wang, Z.L., *Appl. Phys. Lett*. **2002**, *81*, 1869.

[24] Moon, C. S.; Kim, H.-R.; Auchterlonie, G.; Drennan, J.; Lee, J.-H., *Sens. Actuators B* **2008**, *131*, 556.

[25] Jing, Z.; Zhan, J., *Adv. Mater.*, **2008**, *20*, DOI:10.1002/adma.200800243

[26] Dai, Z. R. ; Pan, Z. W. ; Wang, Z. L., *J. Am. Chem. Soc.* **2002**, *124*, 8673.

[27] Batzill, M.; Chaka, A.M.; Diebold, U., *Europhys. Lett.*, **2004**, *65*, 61.

[28] Comini, E. ; Guidi, V. ; Malagu, C. ; Martinelli, G. ; Pan, Z. ; Sberveglieri, G. ; Wang, Z.L., *J. Phys Chem. B* **2004**, *108*, 1882.

[29] Hernández-Ramírez, F.; Tarancón, A.; Casals, O.; Arbiol, J.; Romano-Rodríguez, A.; Morante, J.R., *Sens. Actuators B,* **2007**, *121*, 3.

[30] Huang, X.; Lee, W.-C.; Kuo, C.; Hisamoto, D.; Chang, L.; Kedzierski, J.; Anderson, E.; Takeuchi, H.; Choi, Y.-K.; Asano, K.; Subramanian, V.; King, T.-J.; Bokor, J.; Hu, C ., *IEEE Int. Electron Devices Mtg. Technical Digest (Washington D.C. Dec.)* **1999**, 67.

[31] Barsan, N., *Sens. Actuators B*. **1994**, *17*,241.

[32] Barsan N. ; Schweizer-Berberich, M. ; Gopel, W., *Fresenius J. Annal. Chem.* **1999**, *365,* 287.

[33] Scott, R.W.J.; Yang, S.M.; Chabanis, G.; Coombs,N.; Williams, D.E.; Ozin, G.A.; *Adv.Mater.***2001**, *13*,1468.

[34] Maiti, A.; Rodriguez, J.A.; Law, M.; Kung, P.; McKinney, J.R.; Yang, P., Nano Lett. 2003, 3, 1025.

[35] Xiong, H. M.; Zhao, K. K.; Zhao, X..; Wang Y.W.; Chen, J. S., Solid State Ionics, 2003, 159, 89.

[36] Liu, Y.; Zhu, W.; Tan, O.K.; Yao, X.; Shen, J. Mater. Sci.: Mater. in Electr. 1996,7, 279.

[37] Epifani, M.; Prades, J.D.; Comini, E.; Pellicer, E.; Avala, M.; Siciliano, P.; Faglia, G.; Cirera, A.; Scotti, R.; Morazzoni, F.; Morante, J.E., J. Phys. Chem. C 2008,112, 19540.

[38] Varela, J. A.; Perazolli, L.A.; Cerri, J.A.; Leite, E. R.; Longo, E., Cerâmica 2001, 47, 117.

[39] Szabo, A.; Ostlund, N. S., *Modern Quantum Chemistry*, Dover Publications, Mineola, NY, **1996**.

TABLES

Adsorbed Site	Adatom Structure	Binding Energy (kcal/mol)	Net Charge Transfer (el)
Oxygen-Vacancy	$[NO_2]_2$	41.4	-0.51
Defect Free Surface	$[NO_2]_1$ $[NO_2]_2$ $[NO_3]_1$ $[NO_3]_2$	11.2 13.8 14.3 25.5	-0.17 -0.17 -0.30 -0.41

$[---]_n$ indicates n single bond(s) to an adsorbed site.

Table1. Summary of the computed binding energy and charge transfer for important adatom structures resulting from NO_2 to the $(10\bar{1})$ surface of SnO_2.

FIGURES

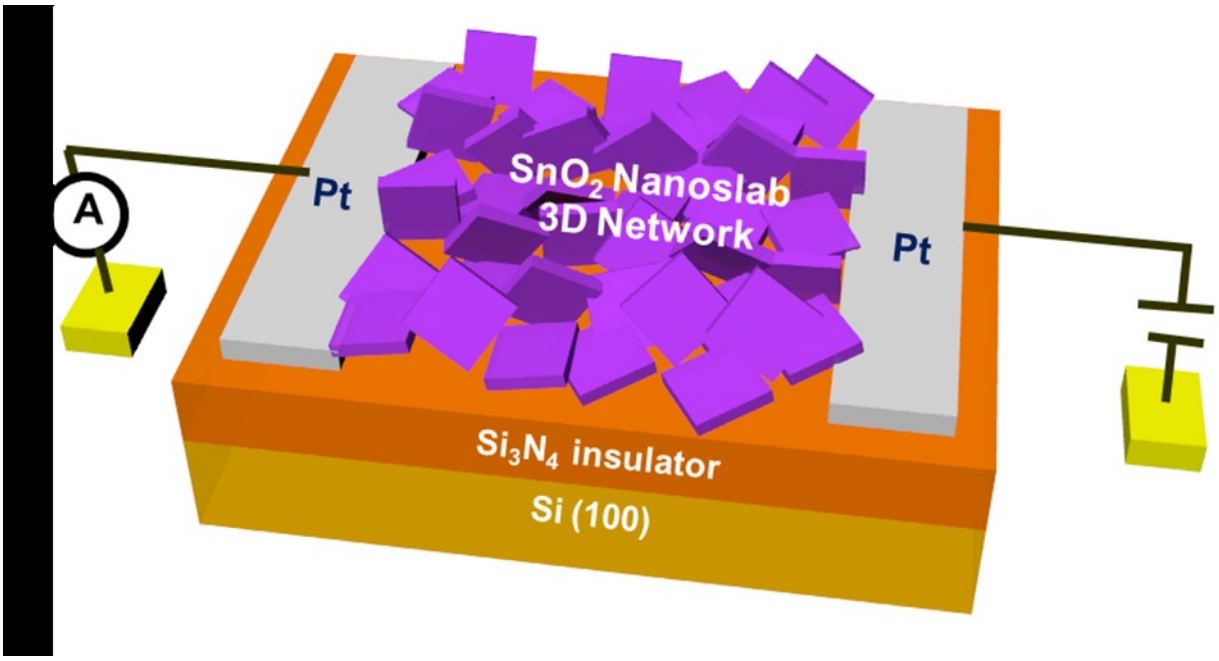

(a)

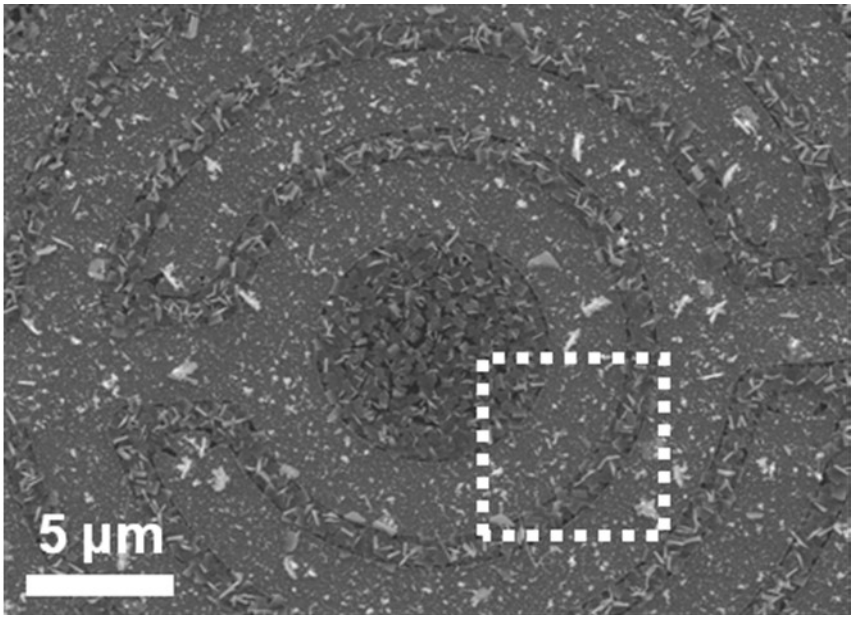

(b)

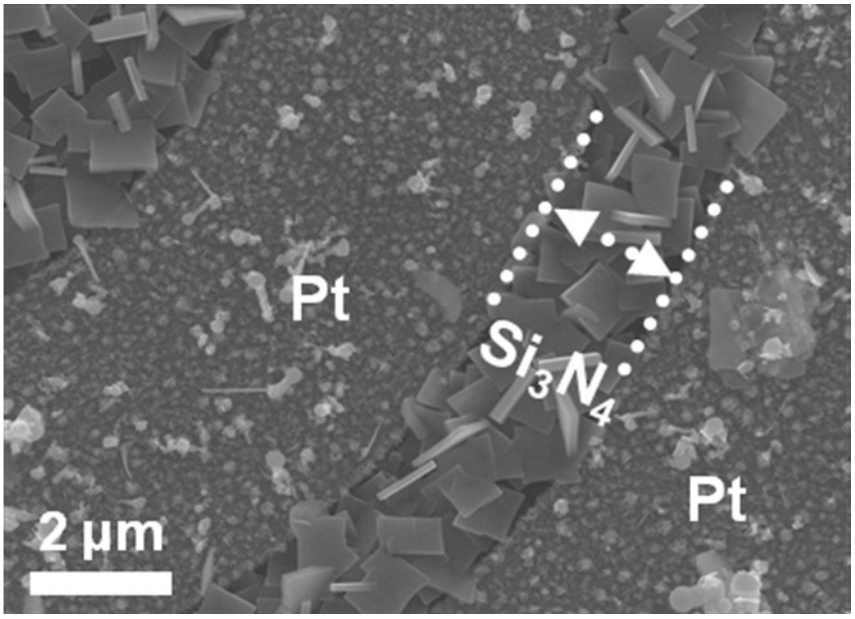

(c)

Figure 1. (a) The schematic diagram of the SnO_2 nanoslab 3D network sensor device. (b) Plan-view FE-SEM image of the SnO_2 nanoslab 3D network synthesized on Pt IDE pattern. (c) Enlarged image of the area within the frame shown in (b).

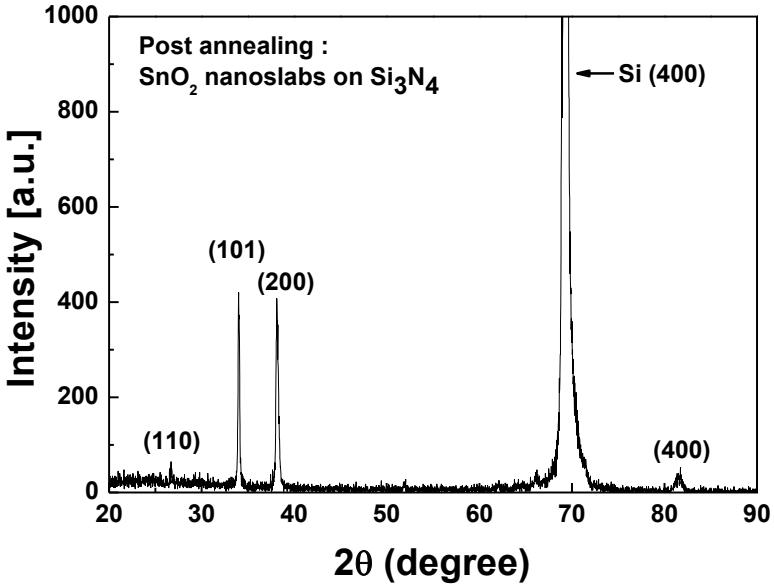

(a)

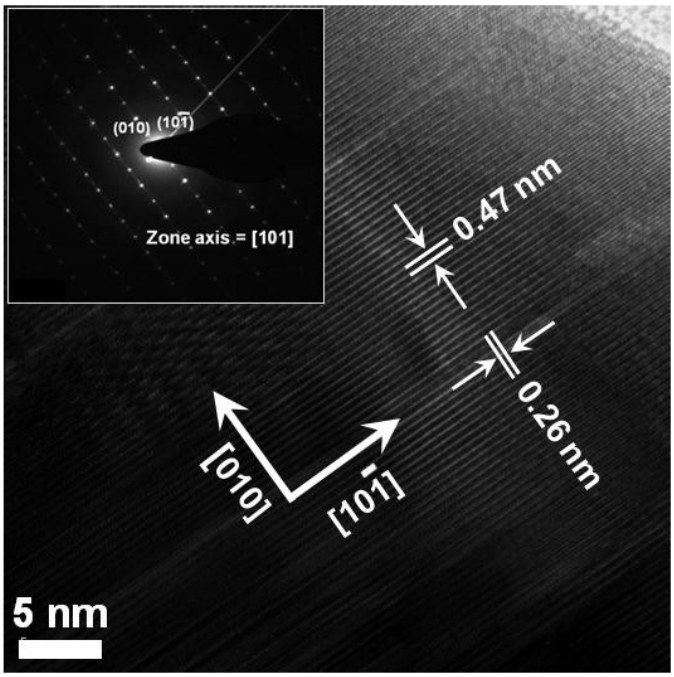

(b)

Figure 2. (a) XRD patterns of a post-thermal annealed SnO_2 nanoslab. (b) HR-TEM image of a post-thermal annealed SnO_2 nanoslab. The inset shows an FFT pattern of the image.

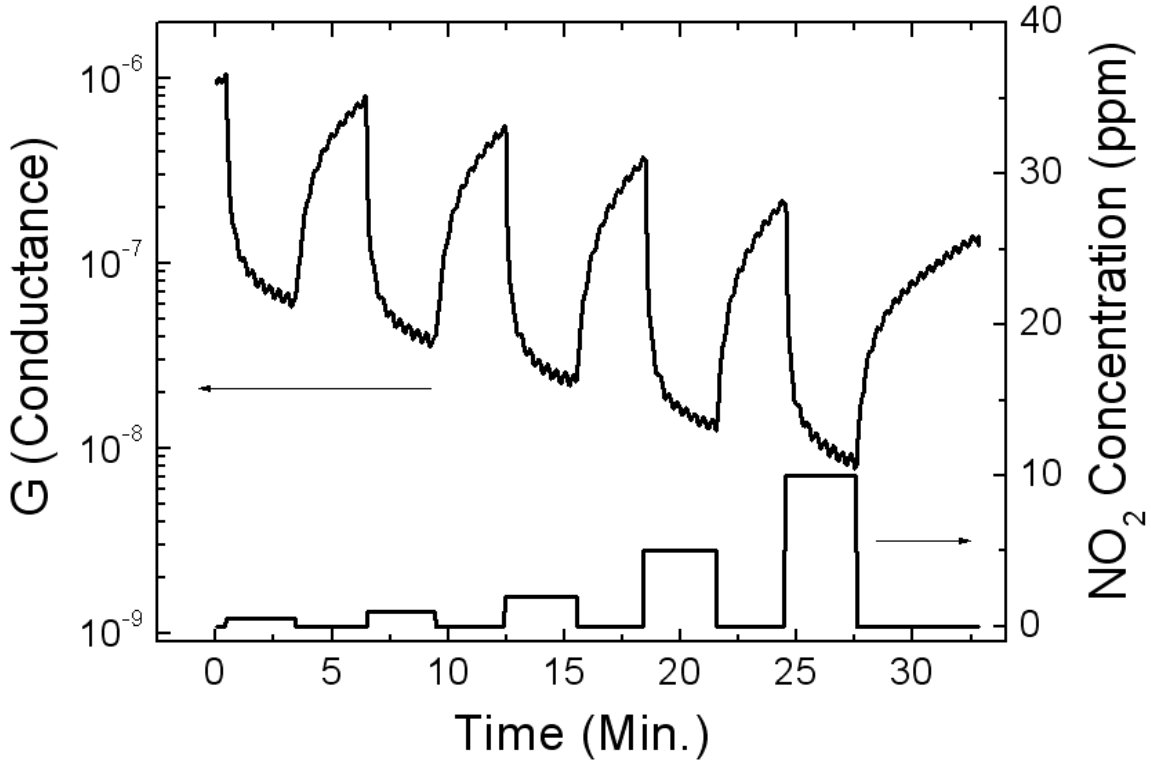

Figure 3. The conductance dependence of a SnO_2 nanoslab network sensor upon cyclic exposure to NO_2 gas with different concentrations at 300 °C.

Figure 4. The low resolution cross-TEM image of SnO_2 nanoslab network prepared by FIB.

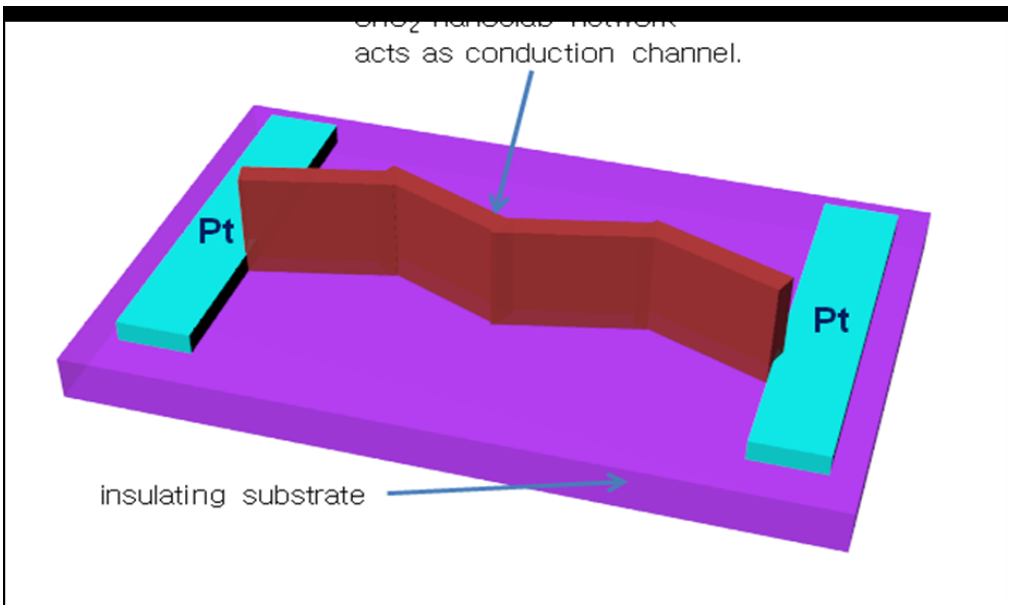

(a)

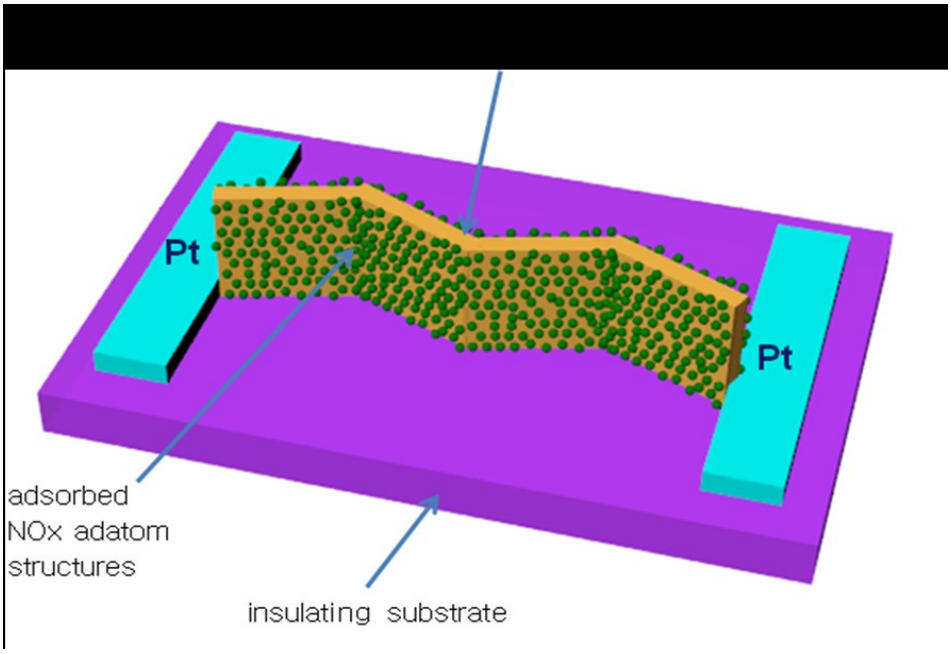

(b)

Figure 5. Schematic diagram explaining the chemical gating of the standing SnO_2 nanoslab network sensor. (a) Before the exposure to NO_2 gas, the nanoslab network acts as conducting channel. (b) After the exposure to NO_2 gas, the network turns into fully depleted region of carriers due to the influence from the adsorbed NOx adatom structures.

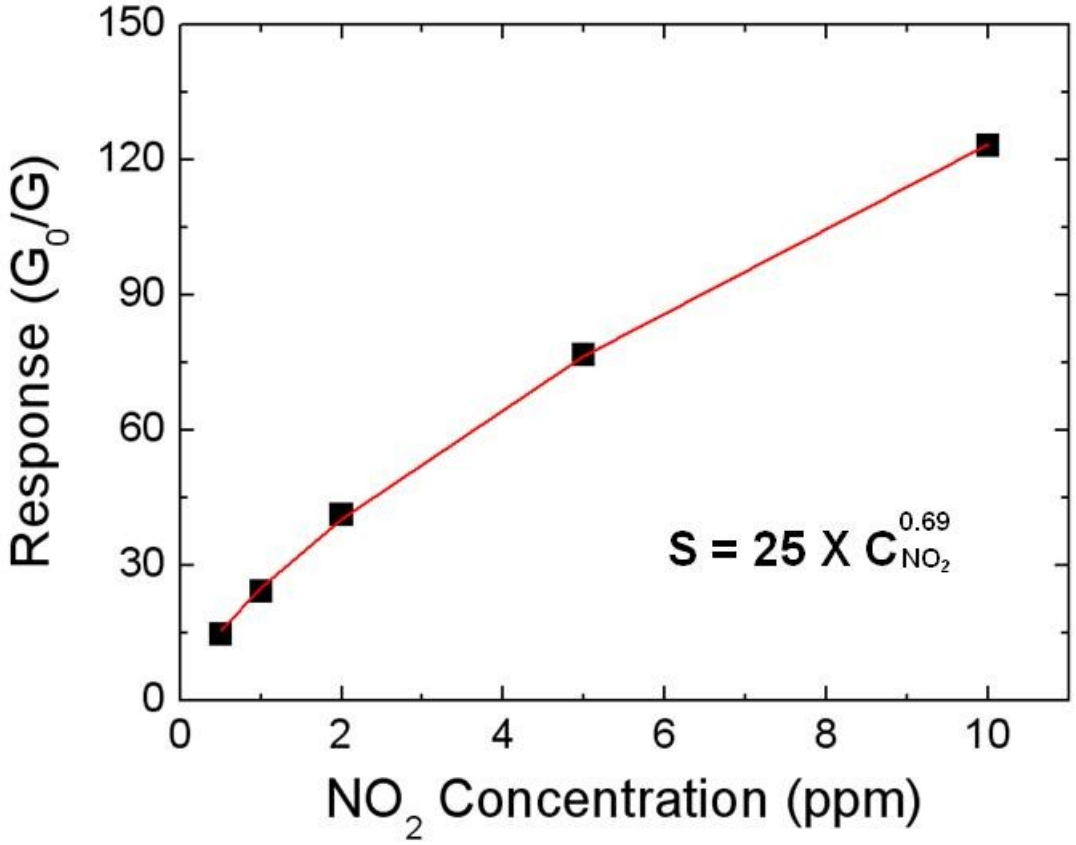

Figure 6. The relationship between the response of a SnO_2 nanoslab network sensor and NO_2 concentration at 300 ^{o}C.